Volume-Of-Fluid Approach for the Characterization of the UWS Spray Breakup Dynamics in the Injector Near- Field

Raul Payri, Gabriela Bracho, Pedro Martí-Aldaraví*, Javier Marco-Gimeno
CMT-Motores Térmicos, Universitat Politècnica de València, Valencia, 46022, Spain
*Corresponding author: pedmar15@mot.upv.es

Abstract
The Injection of Urea Water Solution (UWS) plays a key role in the Selective Catalytic Reduction (SCR) performance and hence in the NOx abatement from Diesel engines. Understanding the main dynamics of such sprays will help in meeting the everyday emission regulations. Computational Fluid Dynamics tools can provide a deeper understanding of the near-nozzle behavior of such sprays. An Eulerian-Eulerian framework known as Volume-Of-Fluid (VOF) has been applied to a commercially available UWS injector. Together with it, a Large Eddy Simulation approach has been followed to solve the larger turbulent scales, while modeling the smallest vortexes. Typical injection pressure working condition (corresponding to Re = 4000 and We = 2000) has been simulated for two types of mesh refinement techniques and the results have been post-processed to assess the breakup dynamics of the injected fluid, and to characterize the outcoming droplets (size and velocity) from such phenomenon. The conclusions depict the good agreement on the hydraulic characterization of the injector dynamics between experimental and computational results, as well as a proper match of the Probability Density Function of droplet diameters. It also allowed having a deep insight into the shape of the ligaments and droplets formed, as well as the location where the primary breakup occurs, which has not been properly observed and defined with experimental methods yet. To end up, a VOF index of quality has been proposed for such simulations.

Keywords
CFD, Atomization, Volume-Of-Fluid, LES, UWS.

Introduction

Nitrogen Oxides (NOx) are one of the harmful emissions expelled by Compression Ignited (CI) Internal Combustion Engines (ICE) [1], [2]. In Europe, light and heavy-duty vehicles powered by such engines account for the 39% of the total contribution of NOx into the atmosphere in 2018. Emission regulation entities are continuously narrowing down the amount of permitted NOx products into the atmosphere by means of EURO norms. In order to accomplish such limits both in the present and in the future, active and passive pollutant reduction techniques need to be developed and applied. Selective Catalytic Reduction (SCR) stands as an effective after-treatment technique for NOx abatement in both light and heavy-duty vehicles [3], [4], as well as for maritime purposes. A Diesel Exhaust Fluid (DEF) made of a Urea-Water Solution (UWS) [5] (commonly 32.5% in volume of Urea) is injected into the exhaust pipe, where through droplet evaporation and urea degradation, ammonia gas is obtained, which will reduce the NOx at the catalyst section. The tight spaces and the short times provided for the urea to convert into ammonia can imply that a number of droplets may impinge into the exhaust walls, creating deposits [6], [7] that could negatively affect the engine performance (increasing back-pressure) or not be able to reduce enough amount of NOx. In order to mitigate this phenomenon, it is mandatory to speed up the evaporation process. Spray breakup plays an important role in this matter as the size of the subsequent droplets directly impacts the evaporation of the components. Typically, computational-related studies have employed Lagrangian methods to recreate the spray dynamics after the primary atomization of the jet. From them, the Discrete Droplet Model (DDM) [8] has been widely used for several types of applications. Due to the low injection velocities and therefore low droplet Weber number, it is necessary to initialize the droplet

velocity and diameter distribution from already experimentally-characterized injectors, or make use of statistical distribution functions such as the Rosin-Rammler function. To depict such process, Eulerian approaches allow to have an insight of the jet disintegration and characterize the ligaments and droplets formed out of the spray core which would be considerably hard to measure by experimental means.
The purpose of this work is to recreate the primary atomization behavior of an UWS injector, but using pure water instead of DEF, as there is an increasing trend in using such fluid to characterize low-injection-pressure devices and to avoid deposit formation on test rigs. For that, a Volume-Of-Fluid approach will be used to depict the internal flow dynamics of the injector itself.
The present document will be divided into the following sections: the introduction, where a brief state-of-the-art is described, methods, where the geometry will be presented and the equations to solve, the section where the main findings are included, and finishing with the main conclusions extracted.

Material and Methods

The commercial CFD package CONVERGE v3.0 has been used to perform the spray simulations. A three $150\,\mu\mathrm{m}$ co-planar hole UWS injector has been recreated by employing a CT scan. From it, the main features of the injector body have been included in the computational model. A further geometry description is included in a previous study [9]. Both the gas and the liquid phases are treated in an Eulerian way. Apart from solving the continuity, momentum and energy transport equations [9], the volumetric void fraction equation is included (Equation 1). It stands as the ratio between the volume of the gas phase to the total volume in each one of the cells of the domain, where a value of $\alpha = 0$ means a cell filled with liquid, while $\alpha = 1$ indicates a gas-filled cell.

$$\frac{\partial \alpha}{\partial t} + u \cdot \nabla \alpha = 0 \tag{1}$$

Then, the density and viscosity of each cell are calculated based on the volumetric void fraction with a linear relationship.
A Large Eddy Simulation (LES) approach has been taken. The larger eddies are resolved, while the small scales are modeled through Sub-Grid (SGS) models. This separation is done using a spatial filter, which usually on Finite Volume Methods (FVM) is the grid itself. The residual stresses are modeled by an Eddy Viscosity Model. A Dynamic Smagorinsky SGS model has been used for such purpose. The Werner and Wengle wall model is employed to calculate the appropriate variable values at the closest cell to the walls. The equations have been numerically solved with a Pressure Implicit with Splitting Operator (PISO) method. A convergence tolerance of 1e-6 has been used for momentum and energy equations, while a value of 1e-5 has been set for both pressure and density. These equations have been solved with a SOR approach except for the pressure equation, which has taken the BICGSTAB method.
Due to the cell count requirements for a VOF approach capable of detecting small enough droplets, only a section of the injector has been retained, and therefore one of the three nozzles will be simulated. The result of that geometry reduction is seen in Figure 1. The fluid domain has been discretized by a cartesian mesh, and a base size of $65\,\mu\mathrm{m}$ has been selected.
Two types of meshing approaches have been followed, leading to two different simulations. In the first approach, a Fixed Refinement (FR) mesh has been created. To deal with the smaller gaps located in the injector and where the spray is expected once injected, several fixed refinement regions have been introduced within the injector itself, and in the discharge volume region. The resulting cell size is calculated according to $L = L_{base}/2^p$, where p is the refinement level. The smallest size is achieved at the injector nozzle and in the location where the spray is expected, with a refinement level of 5. The resulting mesh has a total cell count of approximately 24 M. This allows capturing a minimum droplet size of $4\,\mu\mathrm{m}$ in the discharge volume region close to the nozzle. A close-up of the nozzle region in Figure 2a.

The second approach relies on the Adaptive Mesh Refinement (AMR) for refining the zones where the spray is located. This mechanism allows to temporally refine the mesh locally while the simulation is running in the zones where a higher flow variable gradients are obtained. Therefore at the time of the initialization, only mesh refinements will be located within the injector itself to properly capture the velocity gradients. In the discharge volume region there are no initial refinements, but when the fluid is introduced into it, local refinements are introduced to properly characterize the ligaments and droplet shapes. For that, an AMR refinement depending on the velocity gradients is introduced up to a refinement level of 3, while the volumetric liquid fraction has an AMR refinement level up to 4. Based on this, the cell count prior to the spray injection is 2.5M, while when quasi-steady-state conditions are reached, a total cell count of 9M is achieved. A snapshot of the AMR-based refinement is shown in Figure 2b.
The combination of AMR techniques and LES simulations is known to induce theoretical errors related to the commutativity property of the differencing and filtering operations. Commutativity is only achieved when the filtering operation to remove small scales has a constant width, and therefore LES equations would have the same form as the unfiltered N-S [10]. To quantify the possible errors introduced by this approach, an LES quality parameter has been computed and analyzed.

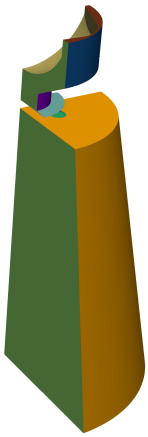

Figure 1. The geometry of the injector cut used for simulation purposes.

The injector has been initialized with pure water down to the nozzle exit at a temperature of $300\,\mathrm{K}$, while the discharge volume is filled with air at $623\,\mathrm{K}$. The pressure of the water-filled

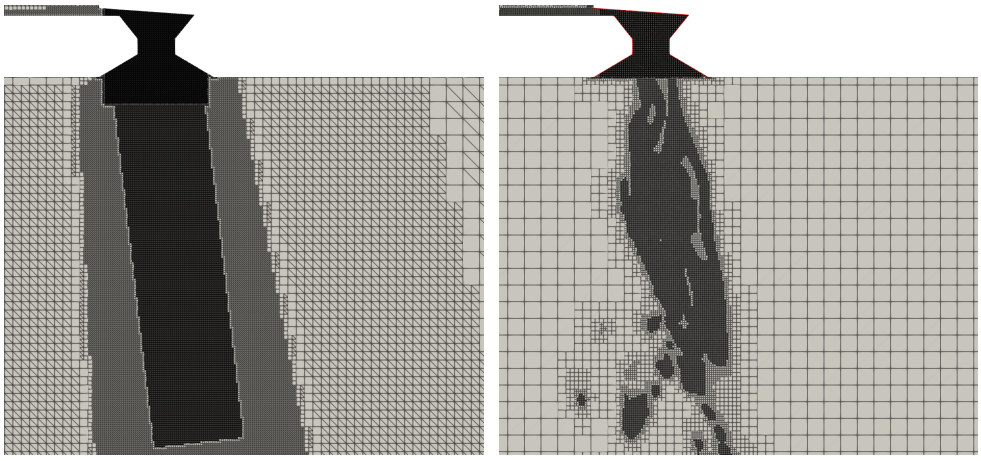

(a) Fixed Refinement (b) AMR Refinement

Figure 2. Mesh snapshot for the two types of refinement techinques employed.

region is set to $9\,\mathrm{bar}$, while the air-filled zone has an initial pressure of $1\,\mathrm{bar}$. When it comes to the boundary conditions, the upper side of the injector has been set as a total pressure inlet, with the same pressure as the initialization condition ($9\,\mathrm{bar}$). This corresponds to a Re = 4000 and We = 2000, leading to a second wind induced breakup regime. The sides of the injector have been set as walls. All the sides of the discharge volume are set as pressure outlet conditions with a value of $1\,\mathrm{bar}$, except for the upper side of the volume, which has been set as a wall. A symmetry condition has been imposed to the surfaces that are present due to extracting a section of the injector circumference.

A LES quality parameter has been implemented, proposed by Pope [11]. It relates the resolved turbulent kinetic energy to the total kinetic energy of the flow field. The total turbulent kinetic energy (TKE) is obtained by the sum of the resolved part plus the modeled part. The resolved TKE depends on the filtered velocity fluctuations of each component (Equation 2), while the modeled turbulent kinetic energy is obtained based on the sub-grid viscosity ν_{SGS} (Equation 3).

$$k_{res} = \frac{1}{2}\left(u_{RMS}^2 + v_{RMS}^2 + w_{RMS}^2\right) \quad (2) \qquad k_{mod} = \frac{\nu_{SGS}^2}{C_m^2 \Delta_e^2} \quad (3)$$

For the simulation set with a fixed embedding, an overall IQk value of 0.8 has been obtained for most of the computational domain. Certain zones with low IQk values are observed mostly on the inside of the injector, where velocities are almost negligible. Once a velocity gradient starts to build up, the IQk value quickly rises to acceptable values. The simulation with the AMR approach also shows similar quality contours, reaching satisfactory overall qualities.

Results and Discussion

Validation

Validation of the results has been done based on hydraulic results obtained from experimental means. Such experimental results have been extracted from the ROI characterization performed by Payri et al. [12]. The results of such validation have been included in Table 1, showing good agreement in ROI results (< 1%).

	ROI	ROI Error
Experimental	$1.102\,\mathrm{g\,s^{-1}}$	-
Fixed Refinement	$1.092\,\mathrm{g\,s^{-1}}$	0.92%
AMR Refinement	$1.106\,\mathrm{g\,s^{-1}}$	0.42%

Table 1. ROI results for the experiment and the LES-VOF simulation for $8\,\mathrm{bar}$ of injection pressure, and the error with respect to the experimental output.

Flow Morphology

The influence of the mesh has been first assessed by representing the flow structure and thresholding the solution by the values of the volumetric void fraction. Figure 3 shows a temporal snapshot of the solution at 1 ms of simulation time. Significant differences are observed in the jet structure. Fixed meshing strategy shows a uniform breakup along the discharge volume with a very distinct droplet formation structure at the middle of the domain, creating quite a uniform set of droplet sizes. The associated velocities of those structures quickly slow down after injection to 15 m/s, while detached droplets show even lower velocities close to 7 m/s. On the other hand, the solution of the AMR technique shows an increased breakup behavior, observing more detached droplets and ligaments, as well as a wide range of droplet sizes. In addition to it, the velocities extracted are larger, as the long ligaments that have not detached from the main jet show velocities close to 30 m/s, and although the breakup droplets show also lower velocities, they show values larger than 10 m/s. Additionally, the FR case shows no complete spray breakup before exiting the domain, while the AMR approach depicts jet breakup at around 4 mm down the nozzle exit.

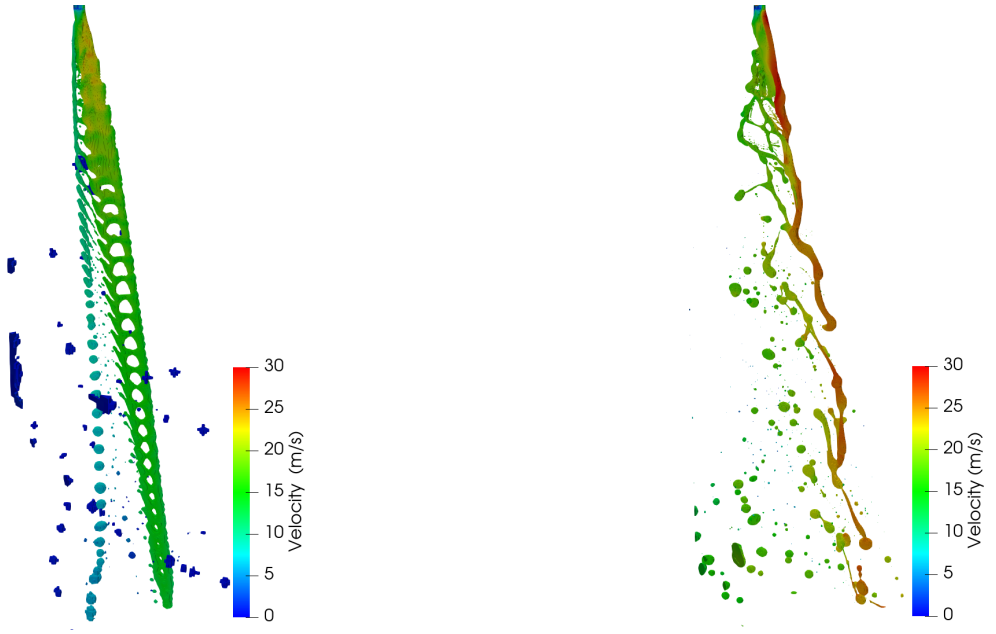

(a) Fixed Refinement (b) AMR Refinement

Figure 3. Temporal snapshot of the threshold on the cells with a Void Fraction < 0.5 for the two mesh refinement approaches.

Atomization

To assess the atomization process a postprocessing routine has been applied to differentiate between the liquid jet and the droplets using a connectivity filter. To extract the diameter of the resulting droplets, the volume of the cells that compose each droplet has been summed up, and the diameter of a sphere with equivalent volume has been obtained. When it comes to calculating the velocities, a mass averaged velocity has been obtained from the cells that compose each droplet. Probability Density Functions (PDF) of the droplet size and injector-axis velocities have been obtained for each temporal snapshot and an average has been computed (Figure 4a). Clear effects between the two types of mesh refinement are detected. FR techniques show slightly higher droplet diameters than the AMR approach. FR shows a peak of diameters at $17\,\mu\mathrm{m}$, while AMR shows a peak at $7\,\mu\mathrm{m}$. In the FR case, droplets that might move away from the refinement cone to larger cells might be under-solved or their shape could be misrepresented, while AMR allows to keep refining locally the mesh to properly capture their shape, therefore allowing to capture smaller droplets and displacing the peak towards the left. Experimental values under cross-flow conditions show similar Probability values (0.05) at $16\,\mu\mathrm{m}$ [13].

Results for the velocity PDF are shown in Figure 4b. In concordance to what was seen in the temporal snapshots of the liquid cells, the FR simulation shows lower velocities compared to the AMR approach. Droplets leaving the refinement cone in the FR simulation might be represented with too few cells, and therefore by not capturing properly the droplet interface, errors could be computed when it comes to the velocity.

To identify if the FR simulation is able to solve most of the droplet structures of the simulation and to confirm that the velocity PDF results might be affected by this under-solving effect, a quality index has been proposed according to the ratio of solved droplet mass to total droplet mass of the droplets, Equation 4. A resolved droplet is defined as the droplet that has a equivalent diameter of 6 grid cells [14]. Table 2 shows the results of such index for a temporal snapshot at 2 ms ASOI. Having the FR simulation a 20% lower $\mathrm{IQ_{VOF}}$ and more than twice the amount of elements, the AMR approach is recommended for such purposes, and therefore

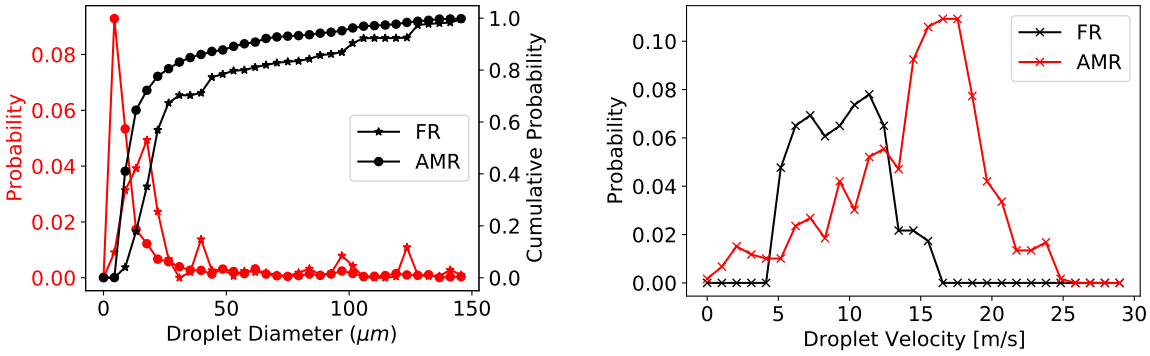

(a) Diameter PDF

(b) Velocity PDF

Figure 4. Number-Based PDF and cumulative PDF of the droplets diameter at for the two simulations performed (a) and the axial velocity PDF for both simulations (b).

only this simulation will be used for characterizing the breakup regime as it is more reliable.

$$IQ_{VOF} = 1 - \frac{m_{undersolved}}{m_{total}} \tag{4}$$

Simulation	$\mathrm{IQ_{VOF}}$
FR	0.798
AMR	0.989

Table 2. Index of Quality proposed for VOF results applied to the two types of meshing strategies employed for a specific time step.

Breakup Regimes

The breakup regimes of the simulations can be analysed by means of non-dimensional numbers. We-Re and Oh-Re charts have been extracted for the AMR simulation as it has shown so far better droplet resolution and hydraulic characteristics closer to experiments. For each one of the droplets detected in the domain, the corresponding numbers have been calculated. For Figure 5a, the Weber number related to the gas has been plotted against the Reynolds number, and it shows how small the We number is, and therefore no secondary breakup should be expected [15]. From Figure 5b, the Oh number has been calculated, and the several breakup regimes have been included in it. The jet can be identified to work in the boundaries of First and Second wind induced regimes, while most of the droplets fall in the Rayleigh breakup region and on the First Wind Induced regime. This information is useful to initialize DDM simulations with VOF droplet distributions instead of using a pre-defined Rosin Rammler function. In addition to that, the breakup outcomes could be used to modify existing DDM breakup models in order to recreate the primary breakup without the need of using expensive methods as Eulerian-Eulerian VOF.

Conclusions

In this study, a UWS injector has been simulated under typical working conditions and with two types of meshing approaches, FR and AMR. A preliminary validation of the simulations against experimental data has been done with respect hydraulic parameters such as the ROI. Both methods allow a proper characterization of the mass flow rate of the injector. The larger turbulent scales are properly solved as a good LES quality index is achieved through the domain. With respect to the jet breakup, significant differences in the jet morphology are observed, as well in the droplet size PDF, indicating that the AMR approach allows to better resolve the

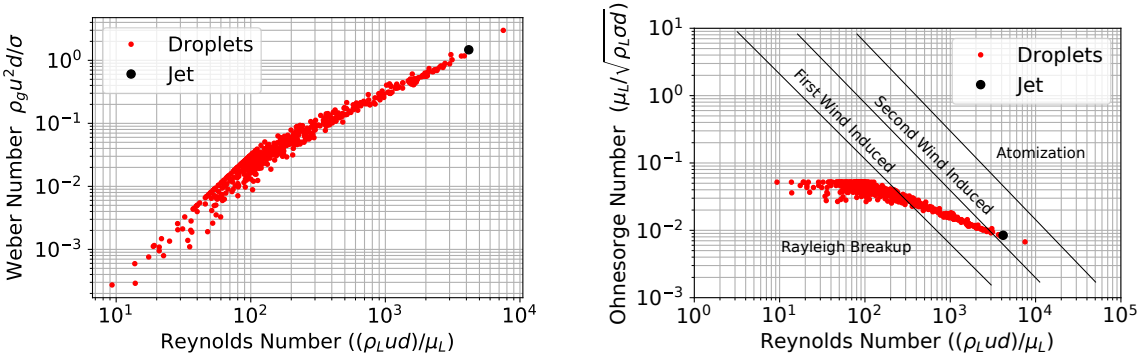

(a) Weber-Reynolds

(b) Ohnesorge-Reynolds

Figure 5. Diagrams non dimensional numbers for the AMR approach.

smaller droplets. Velocity distributions are also affected by the mesh approach because of the amount of under-solved droplets. A new Index Of Quality confirms that the FR simulation shows a larger fraction of the droplet mass that is not properly solved. From these results, it can be assessed that the use of AMR approaches for solving the spray breakup dynamics in a LES simulations seems to be more realistic than employing FR meshes where the computational cost increases significantly if most of the droplets need to be resolved.

Acknowledgements

We gratefully acknowledge the computing resources provided on Bebop (and/or Swing and/or Blues), a high-performance computing cluster operated by the Laboratory Computing Resource Center at Argonne National Laboratory. Additionally, the Ph.D. student J.M.-G. has been funded by a grant from the Government of Generalitat Valenciana with reference ACIF/2020/259 and financial support from The European Union.

Nomenclature

UWS Urea Water Solution
CFD Computational Fluid Dynamics
VOF Volume-Of-Fluid
DEF Diesel Exhaust Fluid
ROI Rate Of Injection
FR Fixed Refinement
AMR Adaptive Mesh Refinement
BICSTAB Biconjugate Gradient Stabilized
PDF Probability Distribution Function
SOR Successive Over Relaxation
ASOI After Start Of Injection

References

[1] G. S. Hebbar, “NOx from diesel engine emission and control strategies - a review,” *Int. J. Mech. Eng. & Rob*, vol. 3, no. 4, pp. 471–482, 2014.

[2] E. Dobrzyńska, M. Szewczyńska, M. Pośniak, A. Szczotka, B. Puchałka, and J. Woodburn, “Exhaust emissions from diesel engines fueled by different blends with the addition of nanomodifiers and hydrotreated vegetable oil HVO,” *Environmental Pollution*, vol. 259, 2020, ISSN: 18736424. DOI: 10.1016/j.envpol.2019.113772.

[3] M. Börnhorst and O. Deutschmann, "Advances and challenges of ammonia delivery by urea-water sprays in SCR systems," *Progress in Energy and Combustion Science*, vol. 87, no. August, 2021, ISSN: 03601285. DOI: 10.1016/j.pecs.2021.100949.

[4] B. Guan, R. Zhan, H. Lin, and Z. Huang, "Review of state of the art technologies of selective catalytic reduction of NOx from diesel engine exhaust," *Applied Thermal Engineering*, vol. 66, no. 1-2, pp. 395–414, 2014, ISSN: 13594311. DOI: 10.1016/j.applthermaleng.2014.02.021.

[5] S. Halonen, T. Kangas, M. Haataja, and U. Lassi, "Urea-Water-Solution Properties: Density, Viscosity, and Surface Tension in an Under-Saturated Solution," *Emission Control Science and Technology*, vol. 3, no. 2, pp. 161–170, 2017, ISSN: 21993637. DOI: 10.1007/s40825-016-0051-1.

[6] U. Budziankou, M. Börnhorst, C. Kuntz, O. Deutschmann, and T. Lauer, "Deposit Formation from Urea Injection: a Comprehensive Modeling Approach," *Emission Control Science and Technology*, vol. 6, no. 2, pp. 211–227, 2020, ISSN: 21993637. DOI: 10.1007/s40825-020-00159-x.

[7] H. Smith, T. Lauer, M. Mayer, and S. Pierson, "Optical and Numerical Investigations on the Mechanisms of Deposit Formation in SCR Systems," *SAE International Journal of Fuels and Lubricants*, vol. 7, no. 2, pp. 525–542, 2014, ISSN: 19463960. DOI: 10.4271/2014-01-1563.

[8] J. K. Dukowicz, "A particle-fluid numerical model for liquid sprays," *Journal of Computational Physics*, vol. 35, no. 2, pp. 229–253, 1980, ISSN: 10902716. DOI: 10.1016/0021-9991(80)90087-X.

[9] R. Payri, G. Bracho, P. Marti-Aldaravi, and J. Marco-Gimeno, *Mixture Model Approach for the Study of the Inner Flow Dynamics of an AdBlue Dosing System and the Characterization of the Near-Field Spray*, 2021.

[10] A. L. Marsden, O. V. Vasilyev, and P. Moin, "Construction of Commutative Filters for LES on Unstructured Meshes," *Journal of Computational Physics*, vol. 175, no. 2, pp. 584–603, 2002, ISSN: 0021-9991. DOI: 10.1006/jcph.2001.6958.

[11] S. B. Pope, "Ten questions concerning the large-eddy simulation of turbulent flows," *New Journal of Physics*, vol. 6, p. 35, 2004, ISSN: 1367-2630. DOI: 10.1088/1367-2630/6/1/035.

[12] R. Payri, G. Bracho, J. Gimeno, and A. Moreno, "A Methodology for the hydraulic characterization of a Urea-Water Solution injector by means of Spray Momentum Measurement," in *29th European Conference on Liquid Atomization and Spray Systems*, Paris, France, 2019.

[13] G. Bracho, L. Postrioti, A. Moreno, and G. Brizi, "Experimental study of the droplet characteristics of a SCR injector spray through optical techniques," *International Journal of Multiphase Flow*, vol. 135, p. 103 531, 2021, ISSN: 03019322. DOI: 10.1016/j.ijmultiphaseflow.2020.103531.

[14] X. Sun, H. Yan, and F. Chen, "Numerical investigation of atomization of swirling liquid sheets using transforming algorithm," *International Journal of Multiphase Flow*, vol. 152, p. 104 084, 2022, ISSN: 0301-9322. DOI: 10.1016/j.ijmultiphaseflow.2022.104084.

[15] A. H. Lefebvre and V. G. McDonell, *Atomization and sprays*, Second. Boca Raton, FL: Press, CRC, 2017, pp. 17–69, ISBN: 9781498736268. DOI: 10.1201/9781315120911.